JOURNAL OF VIROLOGY, Dec. 2000, p. 11377–11387 Vol. 74, No. 23
0022-538X/00/$04.00+0

Glycoprotein E of Varicella-Zoster Virus Enhances Cell-Cell Contact in Polarized Epithelial Cells

CHENGJUN MO,[1]* EVELINE E. SCHNEEBERGER,[2] AND ANN M. ARVIN[1]

Department of Pediatrics, Stanford University School of Medicine, Stanford, California 94305,[1] and Department of Pathology, Massachusetts General Hospital, Boston, Massachusetts 02114[2]

Received 19 June 2000/Accepted 7 September 2000

Varicella-zoster virus (VZV) infection involves the cell-cell spread of virions, but how viral proteins interact with the host cell membranes that comprise intercellular junctions is not known. Madin-Darby canine kidney (MDCK) cells were constructed to express the glycoproteins gE, gI, or gE/gI constitutively and were used to examine the effects of these VZV glycoproteins in polarized epithelial cells. At low cell density, VZV gE induced partial tight junction (TJ) formation under low-calcium conditions, whether expressed alone or with gI. Although most VZV gE was intracellular, gE was also shown to colocalize with the TJ protein ZO-1 with or without concomitant expression of gI. Freeze fracture electron microscopy revealed normal TJ strand morphology in gE-expressing MDCK cells. Functionally, the expression of gE was associated with a marked acceleration in the establishment of maximum transepithelial electrical resistance (TER) in MDCK-gE cells; MDCK-gI and MDCK-gE/gI cells exhibited a similar pattern of early TER compared to MDCK cells, although peak resistances were lower than those of gE alone. VZV gE expression altered F-actin organization and lipid distribution, but coexpression of gI modulated these effects. Two regions of the gE ectodomain, amino acids (aa) 278 to 355 and aa 467 to 498, although lacking Ca^{2+} binding motifs, exhibit similarities with corresponding regions of the cell adhesion molecules, E-cadherin and desmocollin. These observations suggest that VZV gE and gE/gI may contribute to viral pathogenesis by facilitating epithelial cell-cell contacts.

Varicella-zoster virus (VZV) is a human alphaherpesvirus that causes two diseases, varicella (chicken pox) and herpes zoster (shingles); the latter disease is a recurrent infection following prolonged latency in sensory ganglia. Despite genetic similarities, VZV exhibits an extreme host range restriction in vivo and grows poorly in tissue culture, suggesting that its pathogenic mechanisms differ from those of related herpesviruses. The herpesvirus glycoproteins function at several points in the replication cycle, including viral attachment, entry, envelopment, cell-cell spread, and egress. The VZV glycoproteins gB, gC, gE, gH, gI, gL, gK, and the putative gM have some homology with those of herpes simplex virus type 1 (HSV-1), HSV-2, pseudorabies virus (PRV), and the other nonhuman alphaherpesviruses, but VZV lacks gD and gG (12, 24). Although the spread of VZV is associated with extensive fusion of cell membranes, information about the processes by which VZV and other herpesviruses move to cell junctions, including tight junctions (TJ) as well as adherens junctions, and invade adjacent, uninfected cells is limited. These processes are important for VZV replication, since syncytium formation is a hallmark of VZV infection in vitro and multinucleated polykaryocytes are common in VZV-infected tissues.

The VZV glycoproteins gE and gI form heterodimers and, like the corresponding proteins of HSV and PRV, are likely to be involved in cell-cell spread (3, 4, 15, 19, 30, 56). The functions of VZV gE and the gE/gI complex are of particular interest because, unlike the case for other alphaherpesviruses, gE deletion appears to be incompatible with VZV replication (35). While gI deletion mutants replicate in melanoma cells, intact gI is necessary to achieve the polykaryocyte formation characteristic of VZV infection (35). Full or partial deletion of gI inhibited syncytium formation, altered the conformation and distribution of gE, and reduced infectious-virus yields in melanoma cells (35), and gI was required to generate infectious progeny and to allow normal processing of gE in Vero cells (11).

VZV gE has multiple functions, including Fc receptor activity for nonimmune immunoglobulin G (IgG) (31), binding to mannose-6-phosphate receptors, which may facilitate virus entry, and interaction with the major tegument protein, IE62, which may be involved in virion assembly (58). VZV gE has targeting sequences for the trans-Golgi network (TGN) and is transported from the endoplasmic reticulum (ER) to the TGN in infected and gE-transfected cells (1, 20, 59). VZV gI is also a type I membrane protein that is transported to the TGN and to cellular membranes in VZV-infected and gI-transfected cells (1, 2). In addition, VZV gE may serve as a navigator glycoprotein, forming complexes that direct signal-deficient viral glycoproteins to the TGN (55). Expression of gE using the vaccinia virus-T7 RNA polymerase transfection system indicates that gE undergoes endocytosis from the cell membrane, returning to endosomes and TGN, and recycles back to the cell membrane in a continual trafficking pattern (43, 44). Coexpression of gE/gI in vaccinia virus-infected cells also indicates that gI facilitates gE endocytosis and regulates the trafficking of the gE/gI Fc receptor complex (41).

The purpose of these experiments was to investigate how VZV gE and gI and the gE/gI complex may function in epithelial cells. Epithelial cells are important in VZV pathogenesis because the virus enters the host through respiratory mucosal epithelial cells during primary infection and is transmitted to susceptible contacts following cell-cell spread and virus release from mucosal and cutaneous epithelial cells. Madin-Darby canine kidney (MDCK) cell lines were constructed to express the VZV glycoproteins constitutively. MDCK are polarized epithelial cells in which cellular membrane proteins are restricted to discrete apical and basolateral

* Corresponding author. Mailing address: G-312, Stanford University School of Medicine, 300 Pasteur Dr., Stanford, CA 94305. Phone: (650) 725-6555. Fax: (650) 725-8040. E-mail: cmo@cmgm.stanford.edu.

domains, whereas the same proteins are distributed uniformly on the surfaces of fibroblasts and other nonpolarized cells usually used to investigate VZV replication in vitro. In epithelial cells, cell-cell adhesion and formation of TJ are triggered by Ca^{2+} and are associated with localization of occludin, ZO-1, ZO-2, E-cadherin, and β-catenin to targeted regions of the cell membrane (25, 40). Actin filaments and other cell structural components are also rearranged when these cells become confluent (23). We found that VZV gE expression had multiple effects on MDCK cells. First, it resulted in partial TJ formation under low-Ca^{2+} (LC) conditions whether expressed with or without gI, indicating the capacity to enhance cell-cell contact. Second, VZV gE expression was associated with rapid establishment of TJ gate function, measured by transepithelial electrical resistance (TER) in the presence or absence of gI. As expected, gE expression on cell membranes was limited relative to the intracellular signal, but confocal microscopy suggested colocalization of gE with the cell TJ protein ZO-1. Expression of gE at or near ZO-1 occurred without disruption of normal TJ structures by freeze fracture electron microscopy. However, VZV gE affected the cytoskeleton protein, F-actin, and lipid diffusion in MDCK cells, and these effects on structural components of epithelial cells appeared to be modulated by the coexpression of gI.

MATERIALS AND METHODS

Cells and gE- and gI-expressing cell lines. MDCK clone II/G cells (36) were grown in Dulbecco minimal essential medium (DMEM) supplemented with 10% fetal calf serum (FCS), penicillin, streptomycin, and kanamycin. The gE-expressing cell lines containing the ORF68 gene were constructed by inserting a PCR fragment containing the VZV gE-coding region into TA cloning sites of the pCR3.1 plasmid vector (Invitrogen, Carlsbad, Calif.) to make the plasmid pVZVgE. Similarly, the gI-expressing cell lines containing the ORF67 gene were constructed by inserting a PCR fragment containing the VZV gI-encoding region to make the plasmid pVZVgI. The expression of the cloned genes was driven by the cytomegalovirus (CMV) immediate-early promoter from the pCR3.1 vector. Subconfluent MDCK cell monolayers in six-well cluster plates were transfected with pVZVgE or pVZVgI or both, using the Lipofectin method. The transfected cells were incubated for 48 h and then passaged to Falcon 3803 tissue culture dishes in medium containing 250 mg of G418/ml. After selection for 14 days, surviving colonies were isolated using cloning rings. These stably transfected cells were designated MDCK-gE, MDCK-gI, and MDCK-gE/gI. Genomic DNA from MDCK-gE, MDCK-gI, and MDCK-gE/gI cells was analyzed by PCR using primer pairs gE_f and gE_b and gI_f and gI_b, respectively. G418-resistant MDCK clones that had the expected 1.8-kb ORF68 DNA fragment from MDCK-gE or MDCK-gE/gI and 1.1-kb ORF67 DNA fragment from MDCK-gI or MDCK-gE/gI were expanded in the presence of G418, aliquoted, and stored in liquid nitrogen. Protein expression of gE or gI was assessed by Western blotting and immunofluorescence. Three positive clones of MDCK-gE were obtained from screening 25 cell lines, and 15 clones of MDCK-gE/gI were recovered from 30 screened cell lines. Three MDCK-gE clones and three of the MDCK-gE/gI or MDCK cell lines were used at low passage (<5) for all experiments. The mock transfection control and gE- or gE/gI-expressing cells were grown at low density, trypsinized, and plated onto Transwell filters in medium containing LC (5 μM). Cells were incubated in LC medium for 4 h and then incubated in DMEM-FCS containing normal (1.8 mM) calcium (NC). The cells from all gE- or gE/gI-expressing clones could be maintained in NC-containing medium for up to 5 days with no loss of viability. No differences in viability compared to that of the parent MDCK clone II/G cells were observed. For calcium switch experiments, the MDCK cells were grown at low density and plated onto collagen-coated coverslips or Transwell filters in LC medium for 4 h. Cells were then grown in NC medium (calcium switch) or kept in LC medium up to 3 days. Protein kinase C (PKC) agonist diC8 (1,2-dioctanylglycerol; Sigma, St. Louis, Mo.) at 0.5 mM and PKC inhibitor H7 (1-[5-isoquinolinylsulfonyl]-2-methylpiperazine; Sigma) at 50 μM were added in some experiments.

Construction of plasmids. The entire VZV genome of the Oka strain is contained in four overlapping SuperCos 1 cosmid vectors: pvFsp4 (1 to 33211), pvSpe5 (21875 to 62008), pvPme19 (53877 to 96188), and pvSpe21 (94208 to 124884) (34). ORF67 spans VZV nucleotides 114497 to 115558, while ORF68 extends from nucleotides 115808 to 117676, located within the unique short region in the cosmid pvSpe21. A 6-kb DNA fragment from nucleotides 111911 to 117989 that contained ORF67 and ORF68 was subcloned into the plasmid vector pBS to generate pSac6A (35). The VZV gE open-reading-frame fragment was amplified from pSac6A using primers gE_f and gE_b (5′-ATGGGGACAGTTAA TAAACC-3′ and 5′-CGGTGATCACCGGGTCTTATC-3′). The VZV gI open reading frame fragment was amplified from pSac6A using primers gI_f and gI_b (5′-CGCGATGTTTTTAATCCAATG-3′ and 5′-GTTCTATTTAACAAACGG G-3′). The PCR products were ligated into the pCR3.1 TA cloning vector, yielding the plasmids pVZVgE and pVZVgI.

Antibodies. The antibodies used in these experiments included affinity-purified rabbit anti-ZO-1 antibody (Zymed Laboratories, Inc., South San Francisco, Calif.); rabbit polyclonal anti-α-catenin, anti-β-catenin, mouse anti-gP135, and mouse anti-E-cadherin antibody 3G8 (W. James Nelson, Stanford University, Stanford, Calif.); mouse anti-VZV gE antibody 3B3 and anti-VZV gI antibody 6B5 (Charles Grose, University of Iowa, Iowa City, Iowa); mouse anti-VZV gE antibody 3G8 (Bagher Forghani, California Department of Health Services, Berkeley, Calif.); Oregon Green 488-conjugated phalloidin (Molecular Probes, Eugene, Oreg.); donkey anti-rabbit antibody conjugated with horseradish peroxidase (Amersham, Little Chalfont, Buckinghamshire, England); and affinity-purified fluorescein- and Texas Red-labeled secondary antibodies (Jackson ImmunoResearch Laboratories, Inc., West Grove, Pa.).

Cell extraction, immunoprecipitation, and Western blot analysis. MDCK cells were grown on Primaria tissue culture dishes and extracted in 900 μl of cell lysis buffer (0.1% NP-40, 10 mM Tris [pH 7.5], 1-μg/ml DNase I, 1-μg/ml RNase A, and 1 mM phenylmethylsulfonyl fluoride) on a rocker platform for 15 min at 4°C. Cells were scraped from the plates and centrifuged at 12,500 × *g* for 15 min at 4°C. Supernatants were adjusted with 100 μl of sodium dodecyl sulfate (SDS) immunoprecipitation buffer (1% SDS, 10 mM Tris [pH 7.5], 2 mM EDTA). Protein samples were separated on an 8.5% Laemmli gel and electrotransferred to a nitrocellulose membrane (Immobilon P; Millipore, Bedford, Mass.). First, mouse monoclonal antibody at a dilution of 1:2,000 was used as the probe and detected with donkey anti-rabbit antibody conjugated with horseradish peroxidase (Amersham) at a dilution of 1:4,000. For protein immunoprecipitation, cell lysates were incubated with anti-gE (3B3) or anti-gI (6B5) antibody and immune complexes were separated with protein A–Sepharose CL-4B (Amersham Pharmacia Biotech, Uppsala, Sweden) on a rocker platform overnight at 4°C. After being washed four times with buffers, the immunoprecipitates were analyzed on a 10% polyacrylamide gel and processed for Western blotting as described above.

Immunofluorescence microscopy. Confluent monolayers of MDCK cells were grown on coverslips coated with rat tail collagen or Transwell filters in DMEM-FCS. After 48 h, the cells were washed with phosphate-buffered saline (PBS), fixed with 1% formaldehyde, and permeabilized with 0.2% Triton X-100. Then they were blocked with PBS–0.2% bovine serum albumin (BSA) containing 10% normal goat serum. After a washing with PBS–0.2% BSA, they were incubated with antibodies for 1 h at room temperature. After three washes with PBS–0.2% BSA, the cells were incubated with secondary antibodies (fluorescein isothiocyanate [FITC] anti-rabbit IgG and Texas Red anti-mouse IgG). The coverslips were washed with PBS and mounted in Vectashield (Vector Laboratory, Inc., Burlingame, Calif.). Cells were examined with a Nikon fluorescence microscope using either a 40× lens objective or a Molecular Dynamics MultiProbe 2010 laser scanning confocal microscope. Fluorescence images of stained cells were recorded using Kodak Ektachrome Elite II (ASA 400) films. Developed positive images were then digitized with a slide scanner.

Time course of lipid diffusion in MDCK cells in low-density cultures. Cells were grown for 10, 23, and 47 h. At each time, cells were labeled with the lipophilic carbocyanine tracer CellTracker CM-DiI (Molecular Probes), a phospholipid probe, for 10 min at 4°C. Cells stained with DiI were fixed and permeabilized. The cells were incubated with primary antibody ZO-1 and subsequently washed with PBS-BSA before incubation with goat anti-rabbit IgG and conjugation with FITC. Cells were examined with a confocal microscope.

TER measurement. TER was determined by applying an alternating square-wave current across a cell monolayer on a 12-mm-diameter Transwell filter (Costar, Corning, N.Y.) and measuring the voltage deflection with the Millicell electrical resistance system (Millipore). This device measures confluence quantitatively and assesses cell health qualitatively. TER was measured in three or four filters for all cell lines. TER values were calculated by subtracting the blank values from the filter and the bathing medium and were normalized to the area of the monolayer (filter). Monolayer integrity was monitored after each TER time course study by staining cells with Hoechst 33342 (Molecular Probes). When the control MDCK II/G clone is triggered by calcium switch, TER during the first 24 h ranges from 100 to 250 Ω cm^2 (28).

Freeze fracture electron microscopy. Monolayers of cells grown in 75-cm^2 plastic tissue culture flasks were washed briefly twice with 0.1 M PBS (pH 7.4) and fixed in 2% glutaraldehyde (Ernest F. Fullam, Inc., Schenectady, N.Y.) in PBS for 30 min at room temperature. After rinsing in PBS, cells were removed from the substratum by using a plastic cell scraper (Nunc Inc., Naperville, Ill.). The detached cells were infiltrated with 25% glycerol in 0.1 M cacodylate buffer (pH 7.3), frozen in a liquid nitrogen slush, and freeze fractured in a Balzers 400 freeze fracture unit (Balzers, Liechtenstein). Replicas were cleaned in sodium hypochlorite, washed in distilled water, placed on Formvar-coated grids, and examined with a 301 electron microscope (Philips, Eindhoven, The Netherlands). In a given replica, all TJ images were photographed. The number of TJ parallel strands was counted on electron micrographs by overlaying the area of the TJ with a transparency marked at 1-cm intervals. Since the magnification for all micrographs examined was 62,500×, counts were effectively made at 160-nm intervals. Total TJ length examined by morphometry in each group ranged from 6.4 to 9.4 μm. When the histograms were constructed for the strand frequency,

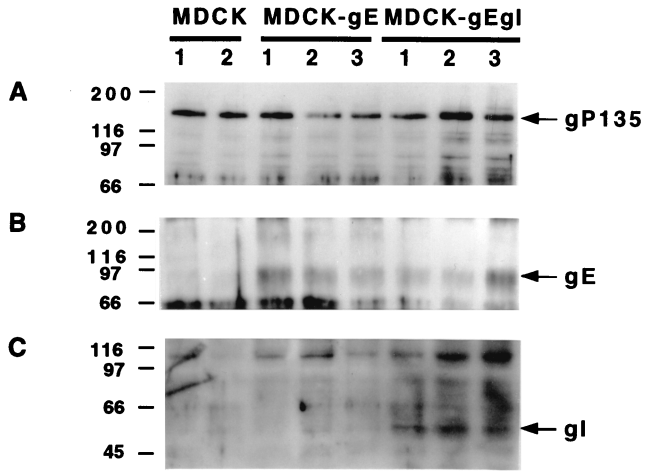

FIG. 1. Western blot analysis of constitutively gE- or gE/gI-expressing cell lines. Two clones of MDCK control cells, three clones of MDCK-gE-expressing cells, and three clones of MDCK-gE/gI-expressing cells were grown on six-well cluster plates for 20 h and then extracted in lysis buffer. Proteins were separated by SDS–8.5% polyacrylamide gel electrophoresis, transferred to nitrocellulose membrane, and probed with anti-gP135 monoclonal antibody (A) or anti-gI monoclonal antibody (C). The same cell lysates were immunoprecipitated with anti-gE monoclonal antibody, separated by SDS–10% polyacrylamide gel electrophoresis, transferred to nitrocellulose membrane, and probed with anti-gE monoclonal antibody (B).

the strand counts were normalized to the greatest total length measured. All freeze fracture experiments were performed and analyzed as a double-blind study.

RESULTS

Expression of VZV gE in MDCK-gE and VZV gEgI in MDCK-gE/gI cells. Three positive clones of MDCK-gE and MDCK-gE/gI along with two MDCK control cell lines were tested for gE and gI expression. GP135, an actin-associated apical membrane protein in MDCK cells (41), was used as a housekeeping protein to assess the loading of each sample (Fig. 1A). Western blotting with anti-gE antibody yielded a 92-kDa protein from MDCK-gE or MDCK-gE/gI cell lysates that was not present in MDCK cell lysates (Fig. 1B). Anti-gI antibody recognized a 55-kDa band in all three MDCK-gE/gI clones tested (Fig. 1C). Clones were chosen for further analysis based upon the consistency of gE/gI protein expression.

To determine the distribution of gE in MDCK-gE clones with or without coexpression of gI, the cells were grown on filters and probed with anti-gE antibody 3G8. In addition to gE, the cellular TJ plaque protein, which is required for TJ integrity, was detected with anti-ZO-1 antibody (27) and cells were stained for E-cadherin, which localizes primarily to the basolateral membrane in confluent MDCK cells (8). Laser scanning confocal microscopy of the clones of MDCK-gE and MDCK-gE/gI cells revealed that most gE was in intracellular sites, as was expected from transient expression of gE in other systems. However, colocalization of gE with ZO-1 along cell membranes was observed (Fig. 2). Confocal XZ sections also indicated colocalization of some gE and ZO-1 in MDCK-gE and MDCK-gE/gI cells (Fig. 2). VZV gE did not appear to colocalize with E-cadherin, which was detected at the same lateral membrane sites in confluent MDCK cells with or without expression of gE or gE/gI (data not shown).

Effects of VZV gE and gI on cell-cell contact and TJ formation. Calcium switch was used to investigate the effect of gE and gI on MDCK cell-cell contact and TJ formation as detected by confocal microscopy (21). E-cadherin belongs to a family of Ca^{2+}-dependent adhesion molecules. As the E-cadherin–catenin complex mediates Ca^{2+}-dependent cell-cell adhesion, E-cadherin becomes localized to the basolateral membranes of MDCK cells (10); removal of calcium makes cadherins accessible to proteases and disrupts cell adhesion (52). As expected, MDCK cells in LC medium showed only occasional staining with anti-ZO-1 antibody at sites of intercellular contact, indicating that no triggering of cell adhesion and TJ formation had occurred. In contrast, ZO-1 was detected in a continuous pattern along the plasma membrane at several sites of intercellular contact after 20 h of incubation of the clones of MDCK-gE or MDCK-gE/gI cells in LC medium (Fig. 3A and B, middle panels; and Fig. 3A, right panel). NC conditions were not required to trigger partial TJ formation by MDCK-gE or MDCK-gE/gI cells. With the "switch" of MDCK cells to NC medium, confluent monolayers were established. And as expected, ZO-1 was detected in a reticular pattern, indicating the translocation of TJ proteins to regions of cell-cell contact in all cell lines. These data suggested that VZV gE has functions that promote cell-cell contact and TJ formation in the absence of Ca^{2+} triggering of E-cadherins (Fig. 3A).

Under NC conditions, E-cadherin binding of extracellular Ca^{2+} triggers the assembly of cell junctions and TJ sealing in monolayers of MDCK cells. Several pathways may be involved in these processes, including the PKC cascade, the calmodulin pathway, and the G protein signaling pathway (5). To determine whether the functional effect of gE on induction of TJ formation was downstream of the PKC cascade, the PKC agonist diC8 or the PKC inhibitor H7 was added to cells in LC medium (6). As expected, diC8 induced partial TJ formation between MDCK cells grown in LC in the control experiments (Fig. 3B, left panel). The PKC inhibitor H7 partially blocked TJ formation between MDCK-gE cells, resulting in a punctate pattern of ZO-1 under LC conditions (Fig. 3B, right panel, arrows). The fact that some TJ formation was maintained indicates that gE functions as more than just a PKC agonist and suggests that there is an alternative pathway for the enhancement of ZO-1 translocation and TJ formation by gE.

When control MDCK cells were triggered to form cell-cell contact by Ca^{2+}-dependent, E-cadherin effects, ZO-1 was localized almost exclusively to sites of intercellular contact. ZO-1 showed its usual very limited expression on membranes that constituted the outer margins of MDCK cells at the edge of the monolayer (Fig. 4). Although the difference could not be quantitated, the consistent observation for all clones of MDCK-gE or MDCK-gE/gI cells was that ZO-1 could be detected more commonly in cell membranes along boundaries where there were no adjacent cells than in control MDCK cells. This observation suggests that VZV gE and gE/gI may have novel effects on the distribution of the TJ protein ZO-1.

VZV gE and gE/gI enhance the establishment of TER. The gate function of TJ, as distinguished from their barrier function, regulates ion and solute diffusion through paracellular spaces (49). The effects of gE and gI on TJ gate function were measured by TER, a test of ion diffusion. The establishment of TER by MDCK-gE, MDCK-gI, MDCK-gE/gI, and MDCK cells was compared at intervals over a 54-h period under LC or NC conditions (Fig. 5). Under LC conditions, TER remained very low in the clones of MDCK-gE as well as in MDCK cells; failure to establish TJ gate function was consistent with the discontinuous ZO-1 staining observed in MDCK-gE and gE/gI cells grown in LC medium (Fig. 3). After a switch to NC medium, the TER of MDCK-gE cell monolayers reached a very high resistance of 420 Ω cm^2 by 20 h (Fig. 5); MDCK cells expressing gE/gI or gI alone also developed high TER in a

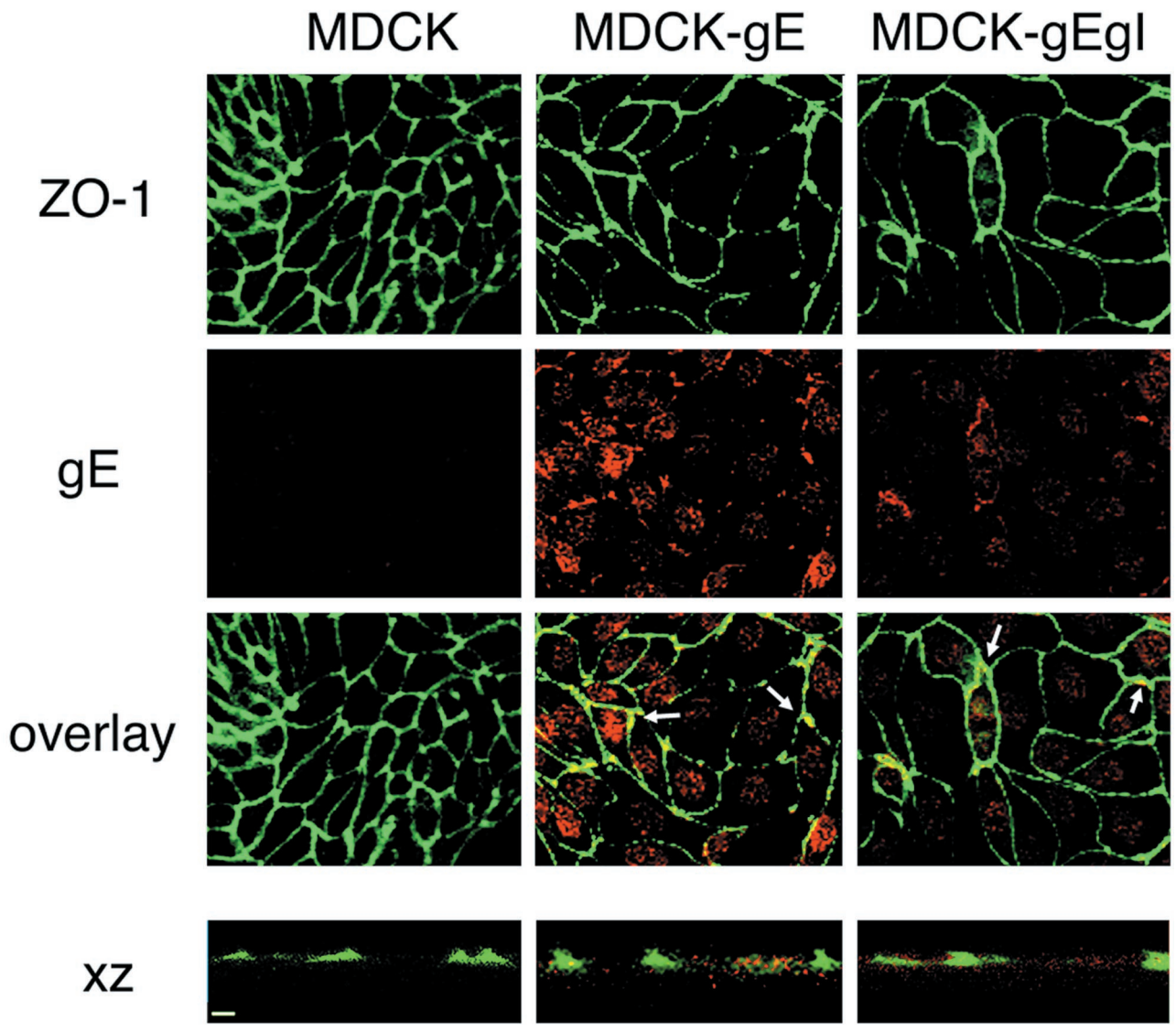

FIG. 2. Immunofluorescence analysis of gE distribution in MDCK-gE and MDCK-gE/gI cells. Clones of MDCK-gE- or MDCK-gE/gI-expressing cells and the MDCK control cells were grown on Transwell filters for 20 h and were fixed and permeabilized. The cells were incubated with the primary antibodies, rabbit anti-ZO-1 or murine anti-gE monoclonal antibody, before incubation with secondary antibodies, goat anti-mouse IgG conjugated with Texas Red or goat anti-rabbit IgG conjugated with FITC. Cells were examined by confocal microscopy. ZO-1 expression; gE staining; and the overlay of ZO-1 and gE staining, visualized by *xy* analysis of cell monolayers, are shown. ZO-1 and gE expression were subjected to *xz* analysis. Bar, 10 μm.

short time. For MDCK-gE, MDCK-gE/gI, and MDCK-gI cells, resistance was sustained at much higher levels than in MDCK cells for up to 30 h; for MDCK-gE clones, it remained above TER for MDCK cells at the last time point of 54 h. MDCK cells expressing gE/gI reached a high maximum TER after approximately 10 h, although the maximum resistance was somewhat lower than that observed in MDCK-gE cell monolayers. To exclude the possibility that the process for generating G418 selected MDCK clones altered the characteristic TER of the parent MDCK II/G clone, cells selected for retention of pTRE, a plasmid that does not express VZV proteins (MDCK-TRE), were tested; both control MDCK cells and the clones of MDCK-TRE showed the expected TER during the first 48 h after calcium switch, ranging from 100 to 250 Ω cm^2 (data not shown). These data suggested that TJ gate function was enhanced in the presence of gE, gE/gI, or gI at early times after cellular confluence was established. Although TER remained significantly higher than in control MDCK cells, interactions between gE and gI appear to modulate the effect of gE alone on TJ gate function in MDCK-gE/gI cells. Based on the acceleration of endocytosis when both gE and gI are present (1, 43), this difference may reflect an increased return of gE from TJ sites to endosomes or to the TGN in gE/gI-expressing cells.

Effect of VZV gE expression on TJ strand organization. In freeze fracture replicas of MDCK-gE cells, the TJ formed a network of interconnected parallel strands present near the apex of the lateral membranes (Fig. 6, lower panel). Its appearance was similar to that in control MDCK cells (Fig. 6, upper panel) (50, 51). These data suggest that the presence of gE near TJ sites or its possible interactions with TJ proteins, such as ZO-1, did not affect TJ strand organization.

Effects of gE and gI on cell morphology, cytoskeletal proteins, and cellular lipids. MDCK-gE and MDCK-gE/gI cells

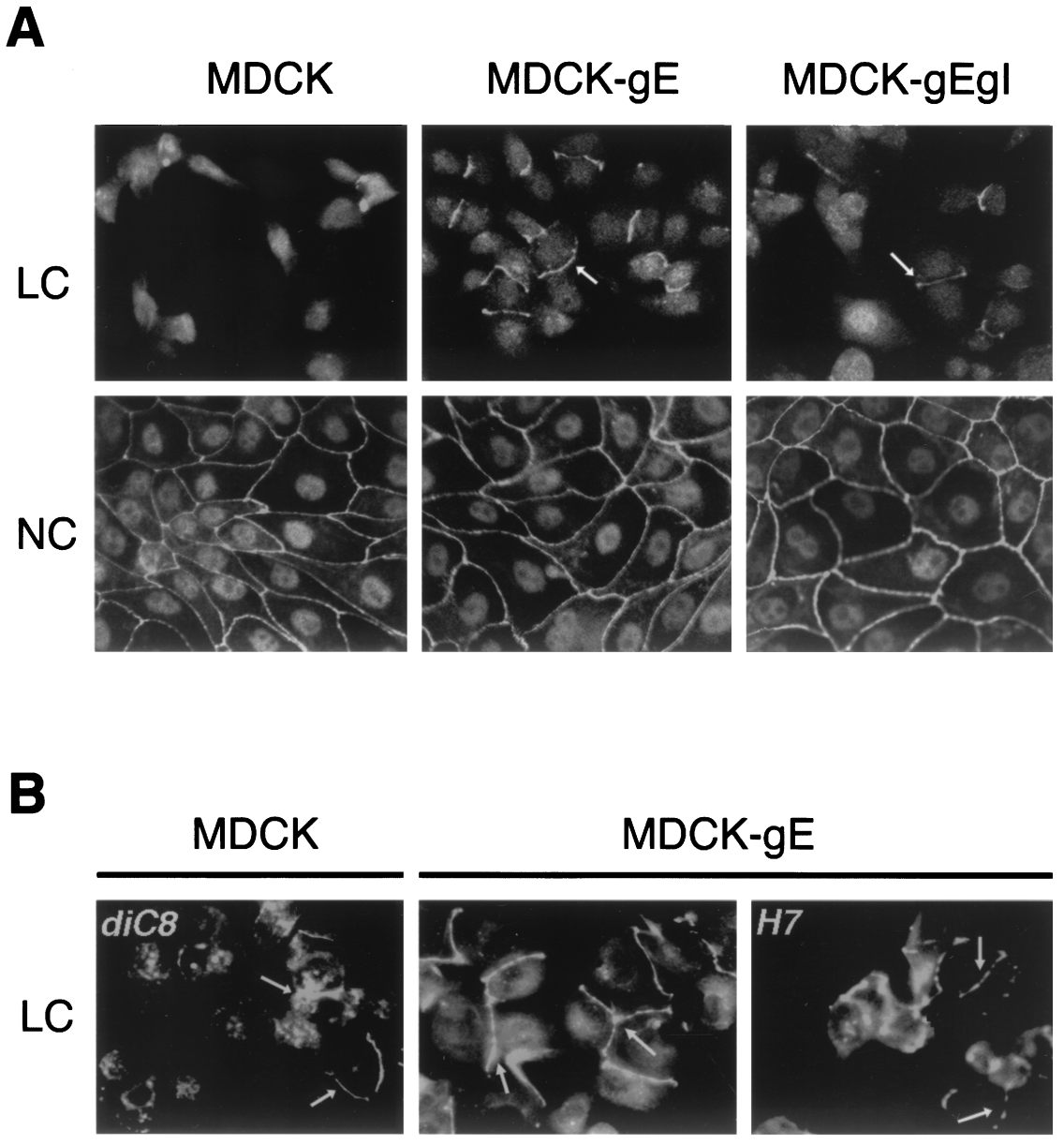

FIG. 3. The effects of VZV gE on cell-cell adhesion and TJ formation. Clones of MDCK-gE and MDCK-gE/gI cells and MDCK controls were grown on glass coverslips in LC or NC medium for 20 h. Cells were fixed and permeabilized before incubation with rabbit anti-ZO-1 and FITC-conjugated anti-rabbit IgG and were examined by confocal microscopy. (A) Membrane staining with ZO-1 is observed at cell contacts between MDCK-gE and MDCK-gE/gI cells but not between MDCK cells under LC conditions; MDCK cells under LC conditions have the characteristic morphology of single cells prior to triggering of monolayer formation by Ca^{2+}. With the switch to NC medium, all cell lines have the expected localization of ZO-1 to cell-cell junctions. (B) diC8, a PKC agonist, permitted some localization of ZO-1 to cell membranes in MDCK cells under LC conditions, and ZO-1 localization in MDCK-gE-expressing cells became extensive; the PKC inhibitor H7 partially blocked TJ formation between MDCK-gE cells, resulting in a punctate pattern of ZO-1 under LC conditions. Arrows, ZO-1 protein.

were consistently larger than the nontransfected controls (Fig. 2). The average number of MDCK cells per microscopic field was 70, compared to 34 for MDCK-gE cells and 32 for MDCK-gE/gI cells. In order to assess whether this difference in morphology was associated with changes in the distribution of cytoskeletal proteins, the cells were stained with Oregon Green phalloidin, a dye specific for F-actin, and evaluated by confocal fluorescence imaging (Fig. 7). The organization of F-actin filaments in MDCK-gE, MDCK-gE/gI, or MDCK cells was scanned in apical to basolateral sections. MDCK-gE cells appeared to be flattened on the substratum compared with MDCK cells, based on the *xz* images (Fig. 7). In contrast to MDCK cells, in which F-actin fibers were lined up in the normal pattern next to cell-cell contacts, F-actin in MDCK-gE cells was localized predominantly in stress fibers at the basolateral regions of the cells and in thick cortical bundles at the periphery. The cytoplasmic region of E-cadherin is anchored to cytoskeletal actin microfilaments through catenins (46). To investigate whether gE might disturb F-actin organization by an interaction with catenins, MDCK-gE cells were examined for colocalization of gE with α-catenin and β-catenin by confocal microscopy. VZV gE did not appear to colocalize with catenin proteins, indicating that gE may alter F-actin distribution by an indirect pathway (data not shown). F-actin organi-

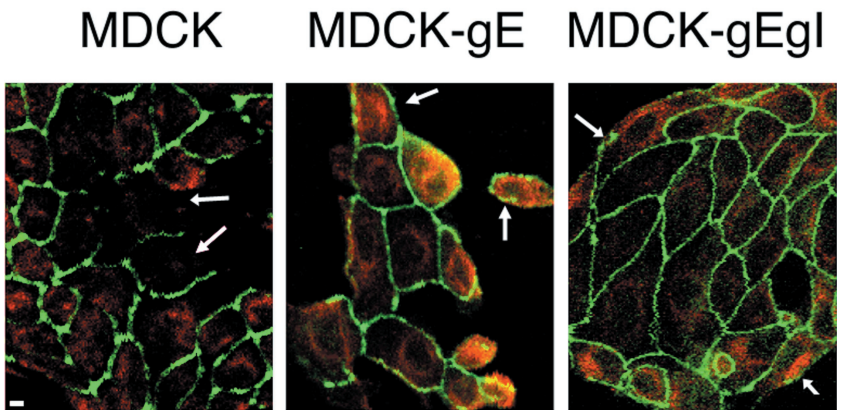

FIG. 4. Effect of expression of gE on ZO-1 and lipid diffusion in low-density cells. MDCK, MDCK-gE, and MDCK-gE/gI cells were grown on coverslips for 23 h. Cells were stained with DiI to identify intracellular lipids, fixed, and permeabilized. The cells were incubated with rabbit anti-ZO-1 before incubation with FITC-conjugated goat anti-rabbit IgG. Cells were examined by confocal microscopy. Bar, 5 μm. Arrows: left panel, cell membranes; middle and right panels, ZO-1 in cell membranes.

zation was similar in MDCK-gE/gI cells and MDCK cells, suggesting that gI binding to gE diminished the disruption of cytoskeletal protein organization induced by gE.

Cellular lipids were stained with CM-DiI and anti-ZO-1 antibody (Fig. 4). At 10 h, staining by CM-DiI was extensive in plasma membranes of all cell lines (data not shown). By 23 h, lipid staining remained somewhat more predominant in the plasma membrane of MDCK-gE cells than in MDCK cells. The pattern of lipid localization in MDCK-gE/gI cells was similar to that observed in MDCK cells; in both cases, lipids were shown to be evenly distributed throughout the cytoplasm (Fig. 4).

Sequence homologies with cadherins and MDCK desmocollin. Computer-assisted amino acid similarity searches (CLUSTALW and Swissprot BestFit) were used to determine relationships between VZV gE and HSV-1 gE and the cell adhesion molecules E-cadherin and MDCK desmocollin (9, 13). The multiple-amino-acid sequence alignment by CLUSTALW and Swissprot BestFit indicated that the extracellular segments of VZV gE, E-cadherin, and desmocollin were similar in size and that these segments had regions of similarity and identity not found in comparing their cytoplasmic components. Two regions of the VZV gE ectodomain, amino acids 278 to 330 and 467 to 498, were shown to have high degrees of similarity (43.4 and 37.5%) and identity (22.6 and 19%) with regions of the cell adhesion molecules E-cadherin and desmocollin. In contrast, HSV-1 gE amino acids 198 to 256 and 403 to 444 had similarities of 25.0 and 11.9% and identities of 10.7 and 4.8% (Fig. 8). The Genetics Computer Group (GCG) GAP program was used to evaluate the significance of the alignment. This program generated the average alignment score ± standard deviation, based on repeated randomized alignments, and this average quality score was compared to the quality score of the actual alignment. VZV gE amino acids 278 to 330 had a significantly higher quality score than E-cadherin by this test (30 versus 15.4 ± 5.6). We speculate that the gE 278-to-330 amino acid sequence might be a functional domain of VZV gE that enhances cell-cell contact, which we observed as partial TJ formation under LC conditions and enhanced maximum TER in gE- and gE/gI-expressing MDCK cells. VZV gE, consistent with a capacity to enhance cell-cell contacts under LC conditions (45), has none of the calcium binding motifs PENE, LDRE, DQNDN, and DAD, which are common in cell adhesion molecules (Fig. 8).

DISCUSSION

This investigation of gE and gI expression in MDCK cells provides initial information about how these VZV proteins may affect the structure and function of polarized epithelial cells. VZV gE expression was associated with the translocation of the TJ protein ZO-1 to cell membranes under LC conditions, whether expressed with or without gI. This effect of gE and gE/gI on the formation of MDCK cell-cell contacts was Ca^{2+} independent, in contrast to the requirement for Ca^{2+} when it is mediated by E-cadherin. While most VZV gE was intracellular in its distribution, evidence of gE colocalization with the TJ protein ZO-1 with or without concomitant expression of gI was suggested by confocal microscopy. In contrast,

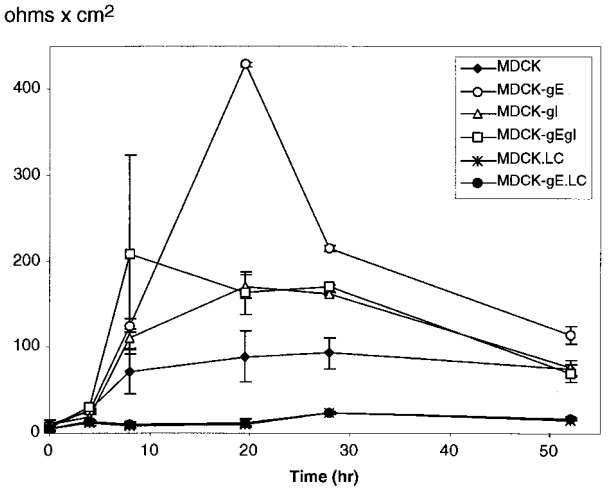

FIG. 5. Development of TER in MDCK cells constitutively expressing VZV gE, gI, or gE/gI. The kinetics of TER was measured sequentially over 54 h in clones of VZV gE-, gI-, or gE/gI-expressing MDCK cells, tested from the time of calcium switch, at time zero to NC conditions. The *y* axis indicates TER, and the *x* axis indicates the time (hour) at which TER was measured. TER measurements are given for MDCK, MDCK-gE, MDCK-gI, and MDCK-gE/gI cell lines in NC medium; measurements were also made with MDCK (MDCK.LC) and MDCK-gE (MDCK-gE.LC) cell lines in LC medium. The data are reported as the means ± standard deviations for three assays. At the end of each experiment, filters were fixed and stained with Hoechst 33342 to confirm the integrity of the monolayer.

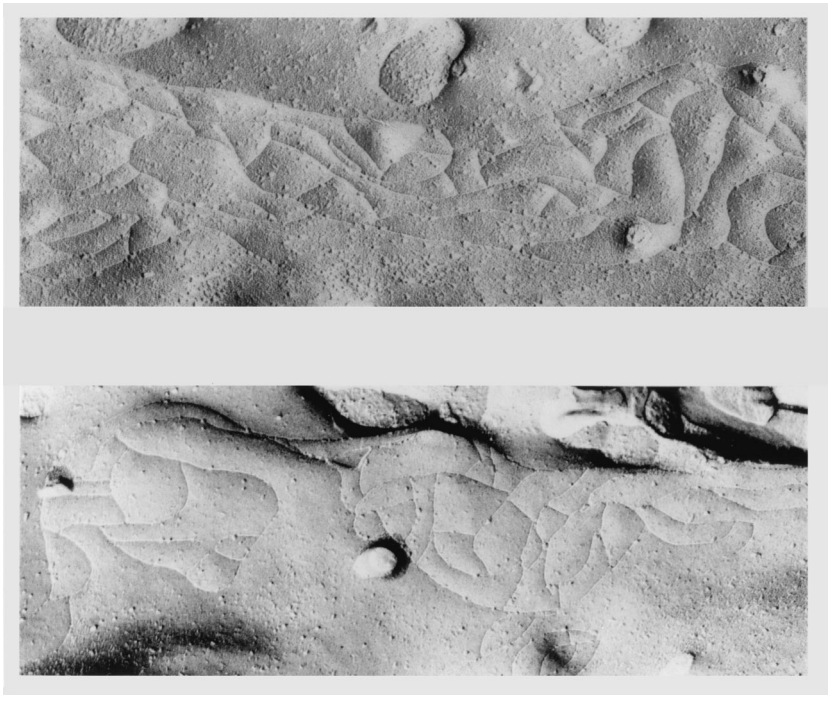

FIG. 6. Freeze fracture electron microscopy of TJ strand organization in MDCK cells expressing VZV gE. The lower panel shows a freeze fracture replica of an MDCK cell stably transfected with gE, demonstrating an exoplasmic fracture face of a representative TJ. The upper panel shows an exoplasmic fracture face of a representative TJ in a nontransfected control MDCK cell. The appearance of the TJ is similar in both cells. Magnification, ×62,500.

the homologous HSV gE protein localized with β-catenin and the glycoprotein encoded by Us9 in the human CMV short unique region were found with E-cadherin when expressed in epithelial cells (15, 16, 33, 34). Experiments assessing TJ gate function demonstrated that VZV gE, gI, and gE/gI expression also accelerated the kinetics of induction and maximum TER in MDCK cells.

Epithelial cell junction proteins move from the ER to form complexes at the plasma membrane that include occludin, ZO-1, ZO-2, cadherins, and catenins (8, 22, 26, 27, 39). When epithelial cells are plated at confluence in calcium-sufficient medium, they adhere to the substrate and form E-cadherin-rich adherens junctions, while occludin and ZO-1 localize to the subapical sites on lateral membranes, forming TJ. As the most apical segment of the intercellular junctions within an epithelial layer, TJ form a regulated seal that restricts paracellular diffusion of ions and solutes and intramembrane diffusion of lipids (21, 32). The E-cadherin–catenin complex is a Ca^{2+}-regulated cell-cell adhesion complex; E-cadherin transport from the ER to lateral membranes is mediated by β-catenin binding to its cytoplasmic domain (10), and catenins anchor E-cadherin to the cytoskeletal protein F-actin (46). ZO-1 mRNA transcription in MDCK cells is also regulated by calcium (22). We found that VZV gE enhanced ZO-1 translocation to cell membranes in the absence of Ca^{2+} triggering, which was observed as partial TJ formation when MDCK-gE cells were tested in calcium switch experiments performed at low cell density. This effect on ZO-1 was maintained when gE was expressed in the presence of gI. The mechanisms by which gE may affect ZO-1 trafficking under LC conditions remain to be determined. Whether gE functions as a PKC agonist like diC8 to facilitate the translocation of ZO-1 or is directly involved in TJ formation, or both, is not certain. Some additional evidence that VZV gE or gE/gI may alter ZO-1 trafficking was provided by the tendency of this TJ protein to appear on cell membranes at the free margin of the monolayer after the calcium switch, while it was rarely found in confluent monolayers of control MDCK cells.

The induction of membrane adhesion between gE- or gE/gI-expressing MDCK cells incubated at low density and under LC conditions suggests that VZV gE may have the capacity to function as a Ca^{2+}-independent adhesion protein to enhance cell-cell contact. Since gE has a large extracellular domain like E-cadherin, one hypothesis is that gE may bind to a cell membrane ligand on uninfected cells in proximity to the infected cell, which could assist viral transport from infected cells. Alternatively or in addition, gE could contribute to the fusion of neighboring cells that were infected independently, since it forms homodimers as well as heterodimers with gI (31, 42); this mechanism would mimic dimer formation by the extracellular domains of E-cadherin (57). Residues 278 to 330 and 467 to 498 in the ectodomain of gE have identities of 22.6 and 18.8% and similarities of 43.4 and 37.5%, respectively, with the corresponding regions of E-cadherin and the MDCK cell adhesion protein desmocollin, but predicted Ca^{2+} binding residues are absent in VZV gE. These similarities between the amino acid sequences of extracellular segments of gE and cell adhesion molecules are only suggestive; whether they actually represent functional domains of gE will require analysis in mutagenesis experiments. However, this possibility is of interest because VZV gE is a substantially larger molecule than its counterparts in other herpesviruses, and its multifunctional nature is becoming well documented (1, 12, 43).

The change in kinetics of induction and peak TER in MDCK cells was a notable and reproducible effect of VZV gE, gI, or gE/gI expression. Although the claudins and occludin are known to be the critical molecules, how they are arranged to form TJ strands is not clear; the molecular mechanisms that

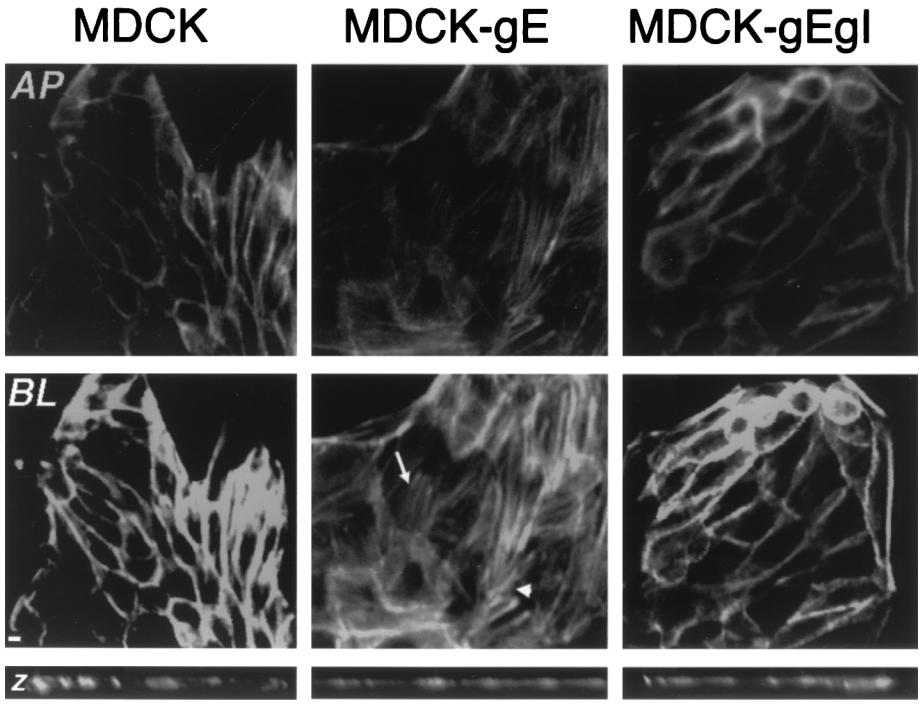

FIG. 7. Effect of expression of gE on cell morphology and F-actin filament distribution. After 24 h of incubation in NC medium, MDCK, MDCK-gE, and MDCK-gE/gI cells were fixed, labeled with 0.165 μM phalloidin, and examined by confocal microscopy. The panels show staining when cell monolayers were examined as *xy* sections, showing the pattern detected at the apical (AP) level (upper row) and the basolateral (BL) level (lower row). Arrow, actin stress fibers; arrowhead, actin in thick cortical bundles. Bar, 5 μm. Narrow panels at bottom show *xz* sections of cell monolayers.

account for the gate functions of TJ remain unresolved, but the regulation of paracellular solute transport is an active process that continues after TJ formation (54). Similar effects on TER were reported with overexpression of occludin or a COOH-terminal truncation of occludin in MDCK cells (7). However, it is not likely that gE or gI has any direct occludin-like functions, since gE and gI are type I transmembrane proteins. By contrast, occludin and the 18 known claudins are all tetraspan integral membrane proteins with both N and C termini in the cytoplasm (49). Extracellular domains of occludin are unique in that they have unusually high tyrosine and glycine content (37). The unusual TER kinetics in MDCK cells expressing gE, gE/gI, or gI is intriguing and indicates that viral proteins may affect TJ regulation of paracellular ion diffusion, but specific pathways cannot be suggested from current information.

In contrast to VZV, HSV-1 gE and gI accumulated at lateral membranes and colocalized with β-catenin in endometrial epithelial (HEC-1A) cells and MDCK cells (17). The human CMV glycoprotein Us9 colocalized with E-cadherin in a basolateral distribution and with F-actin (33). Other differences were that VZV gE trafficked to cell membranes with or without gI in MDCK cells, albeit in limited amounts relative to intracellular concentrations, whereas HSV gE required gI for its translocation to plasma membranes and no colocalization of HSV proteins with ZO-1 was observed. While these various patterns suggest virologic differences, interpretations must be tempered by the fact that these experiments were done using different expression systems and different cellular substrates. Although the effects of VZV gE on ZO-1 localization and TER could be observed in the absence of gI, their occurrence in the presence of gI is important if a functional role in virus-infected cells is to be considered, because gE typically forms heterodimers with gI during VZV replication.

Dingwell and Johnson have suggested that targeting of certain herpesvirus glycoproteins to regions of epithelial cell contact and their interaction with cell junction proteins facilitate the movement of virions into uninfected cells by creating membrane fusion or enable virion release into intercellular spaces, followed by fusion of the viral envelope to the uninfected cell membrane (17). A second hypothesis, which was suggested for human CMV Us9, is that the viral glycoproteins destabilize the cellular proteins that constitute adherens junction complexes, enhancing access to adjacent cells in epithelial tissues by disruption of basolateral membranes (33). We showed that VZV gE and gE/gI complexes did not disturb TJ gate function, as measured by TER. TJ gate function was also preserved in epithelial cells expressing HSV-1 gE and gI (17). Our experiments further demonstrated that TJ strands were structurally intact by freeze fracture electron microscopy. Thus, the evidence is that neither VZV nor HSV-1 gE or gE/gI complexes disrupt the plasma membrane contacts that are generated by cellular proteins. Our experiments indicate that VZV gE and gE/gI actively promoted adhesion of epithelial cell membranes and the establishment of TJ gate function. Although ZO-1 is at the apex of the lateral membrane and β-catenins move to lateral membrane segments below the TJ when MDCK cells are confluent, trafficking of particular herpesvirus glycoproteins to either of these sites could fit the functional model that gE and gI enhance membrane fusion or local release of virions into intercellular spaces next to uninfected cells, as illustrated by Dingwell and Johnson (17). The small-plaque phenotype observed with deletion of VZV gI (11, 35) or with HSV-1 and PRV gE and gE/gI deletion mutants (3, 17, 29, 30) could occur if either fusion or release was impaired. In addition to having pathogenic effects on epithelial cells, the alphaherpesviruses are neurotropic and neuronal cells are also polarized (48). Studies of HSV and PRV gE mutants or mutants that block the formation of gE/gI heterodimers demonstrate that gE and the

```
Length: 53, Percent Identity: 22.6, Percent Similarity: 43.4

VZVgE278-330:     P--PE-----IEP--GVLKVLRTE----KQ--Y-LGVYIWNMRGSD-GTSTYATFLVTWKGDEKTRNPTP
E-cadherin:       PELPDKNMFTINRNTGVISVVTTGLDRESFPTYTLVVQAADLQGE--GLSTTATAVITVT-DT-NDNP-P
Desmocollin:      PNNPR--HFTVHPDTGVITTTTPLLDREKCDTYKLIMEVRDMGGQPFGLFNTGTITISLE-DE-NDNA-P
                  *  *      : :  **  :           * * :    : *   * :: :*   :   *:   *: *

Length: 32, Percent Identity: 18.8, Percent Similarity: 37.5

VZVgE467-498:     DTP---ES--LSGLYVFVVY----FNGHVEAVAYTV-VSTVD
E-cadherin:       DTANWLEINPDTGAISTRAELDREDFEHVKNSTYTALIIATD
Desmocollin:      DEDNWFEINEYTGDLKTVKVLDRE-STFVKNNQYNVSVIAFD
                  *:    *     *    :         :*    *:: :   *


Length: 59, Percent Identity: 10.7, Percent Similarity: 25.0

HSVgE198-256:     PRLP------PPPAPPRSWPSAPEVSHVRGVTVRMETPEAILFSP--GETFSTNVSIHAIAHDDQTY
E-cadherin:       PELPDKNMFTINRNTGVISVVTTGLDRESFPTYTLVVQAADLQGE--GLSTTATAVITVTDTNDNPP
desmocollin:      PNNP--RHFTVHPDTGVITTTTPLLDREKCDTYKLIMEVRDMGGQPFGLFNTGTITISLEDENDNAP
                  *. *          .      :. :.:    *  :      : .   *   : .  *     :*:.

Length: 42, Percent Identity: 4.8, Percent Similarity: 11.9

HSVgE403-444:     PTHGALRLGAVMGAALLLSALGLSVWACMTCWRRRAWRAVKS
E-cadherin:       DTANWLEINPDTGAISTRAELDREDFEHVKNSTYTALIIATD
Desmocollin:      DEDNWFEINEYTGDLKTVKVLDREST-FVKNNQYNVSVIAFD
                     . :.:.   *       *. .    :.     .   . .

LDRE: Ca2+ binding site
```

FIG. 8. Comparisons of amino acid sequences of VZV gE ectodomains and HSV-1 gE extracellular region with those of cell adhesion molecules E-cadherin and MDCK desmocollin. Sequences were compared by CLUSTALW multiple-sequence alignment using the DeCypher bioinformatics supercomputer (Center for Molecular and Genetic Medicine, Stanford University). Two domains from the extracellular region of VZV gE and HSV-1 gE were compared to regions of the ectodomains of E-cadherin and MDCK desmocollin. Symbols: *, amino acid conserved among three proteins; :, amino acid conserved between gE and one of the adhesion proteins; -, gap that was introduced to maintain maximal alignment. Underlined amino acids correspond to the calcium binding motif.

gE/gI complex make a critical contribution to central nervous system spread in animal models, and recent PRV experiments demonstrate that this effect is independent of the gE endocytosis motif (3, 4, 16, 29, 30, 53, 56).

In cellular adherens junctions, cadherins and actin filaments are aligned in bundles with the plasma membrane (38, 52). Viral pathogens, especially poxviruses, have been shown to manipulate cellular cytoskeletal components during replication (14). In contrast to human CMV Us9 protein, VZV gE did not colocalize with E-cadherin or F-actin (33). Nevertheless, VZV gE expression appeared to disrupt the prominent bundles of actin filaments that encircle the lateral membranes in association with adherens junctions and induced the formation of "stress" fibers. Since actin fibers are anchored to cadherins by catenins, gE expression appears to disrupt this complex along the lateral membrane (47). Of note, these changes in actin were independent effects in gE-expressing cells and were not associated with any altered ZO-1 localization, TJ gate function as measured by TER, or TJ structure as visualized by freeze fracture electron microscopy. These marked changes in the cellular cytoskeleton may explain why it has been difficult to generate and maintain VZV gE-expressing cell lines. The yield of MDCK gE-expressing clones was much lower than that of MDCK-gE/gI clones in our experiments. Although gI is dispensable for VZV replication in Vero and melanoma cells, its deletion resulted in a significant decrease in infectious-virus yields, which may reflect the toxic effects of gE on cells when it is not modulated by binding to gI (11, 35). In contrast, the MDCK-gE/gI clones exhibited morphology, F-actin organization, and lipid distribution patterns like those of control MD CK cells. Thus, our experiments suggest that under the normal conditions of VZV infection in which both gE and gI are expressed, their synthesis and intracellular trafficking are associated with preservation rather than with disorganization of the links between membrane cadherins and the actin cytoskeleton in epithelial cells. Cell-cell spread of VZV is associated with the formation of distinctive "viral highways" that disappear when gI is deleted (18, 35). Maintaining membrane and/or cytoskeletal connections through dual expression of gE and gI might be important during the early stages of VZV infection.

This analysis of VZV gE and gI in MDCK cells adds to the accumulating evidence that some herpesvirus glycoproteins may function to enhance contacts between epithelial cells and suggests that these viral proteins have the capacity to facilitate cell adhesion by pathways distinct from those of the Ca^{2+}-dependent E-cadherin-like molecules.

ACKNOWLEDGMENTS

We are grateful to our colleagues who provided necessary reagents and valuable advice, including W. James Nelson, Stanford University; Charles Grose, University of Iowa; and Bagher Forghani, California Department of Health Services. We thank members of the Nelson and Arvin laboratories for their helpful discussions and criticisms and Lee Kozar of the Bioinformatics Resource at Stanford University Medical Center for sequence alignment analysis. We thank Jay Lee for excellent technical assistance.

This work was supported by Public Health Service grant AI20459 to A.M.A. C.M. is the recipient of a postdoctoral fellowship from the VZV Research Foundation.

REFERENCES

1. **Alconada, A., U. Bauer, L. Baudoux, J. Piette, and B. Hoflack.** 1998. Intracellular transport of the glycoproteins gE and gI of the varicella-zoster virus. gE accelerates the maturation of gI and determines its accumulation in the trans-Golgi network. J. Biol. Chem. **273:**13430–13436.

2. **Alconada, A., U. Bauer, and B. Hoflack.** 1996. A tyrosine-based motif and a casein kinase II phosphorylation site regulate the intracellular trafficking of the varicella-zoster virus glycoprotein I, a protein localized in the trans-Golgi network. EMBO J. **15:**6096–6110.
3. **Babic, N., B. Klupp, A. Brack, T. C. Mettenleiter, G. Ugolini, and A. Flamand.** 1996. Deletion of glycoprotein gE reduces the propagation of pseudorabies virus in the nervous system of mice after intranasal inoculation. Virology **219:**279–284.
4. **Balan, P., N. Davis-Poynter, S. Bell, H. Atkinson, H. Browne, and T. Minson.** 1994. An analysis of the in vitro and in vivo phenotypes of mutants of herpes simplex virus type 1 lacking glycoproteins gG, gE, gI or the putative gJ. J. Gen. Virol. **75:**1245–1258.
5. **Balda, M. S., M. L. Gonzalez, R. G. Contreras, S. M. Macias, M. M. Torres, S. J. Garcia, and M. Cereijido.** 1991. Assembly and sealing of tight junctions: possible participation of G-proteins, phospholipase C, protein kinase C and calmodulin. J. Membr. Biol. **122:**193–202.
6. **Balda, M. S., M. L. Gonzalez, K. Matter, M. Cereijido, and J. M. Anderson.** 1993. Assembly of the tight junction: the role of diacylglycerol. J. Cell Biol. **123:**293–302.
7. **Balda, M. S., J. A. Whitney, C. Flores, S. Gonzalez, M. Cereijido, and K. Matter.** 1996. Functional dissociation of paracellular permeability and transepithelial electrical resistance and disruption of the apical-basolateral intramembrane diffusion barrier by expression of a mutant tight junction membrane protein. J. Cell Biol. **134:**1031–1049.
8. **Barth, A. I., A. L. Pollack, Y. Altschuler, K. E. Mostov, and W. J. Nelson.** 1997. NH2-terminal deletion of beta-catenin results in stable colocalization of mutant beta-catenin with adenomatous polyposis coli protein and altered MDCK cell adhesion. J. Cell Biol. **136:**693–706.
9. **Bussemakers, M. J., A. van Bokhoven, S. G. Mees, R. Kemler, and J. A. Schalken.** 1993. Molecular cloning and characterization of the human E-cadherin cDNA. Mol. Biol. Rep. **17:**123–128.
10. **Chen, Y. T., D. B. Stewart, and W. J. Nelson.** 1999. Coupling assembly of the E-cadherin/beta-catenin complex to efficient endoplasmic reticulum exit and basal-lateral membrane targeting of E-cadherin in polarized MDCK cells. J. Cell Biol. **144:**687–699.
11. **Cohen, J. I., and H. Nguyen.** 1997. Varicella-zoster virus glycoprotein I is essential for growth of virus in Vero cells. J. Virol. **71:**6913–6920.
12. **Cohen, J. I., and S. E. Straus.** 1996. Varicella-zoster virus and its replication, p. 2525–2545. *In* B. N. Fields, D. N. Knipe, and P. M. Howley (ed.), Fields virology, 3rd ed. Lippincott-Raven Publishers, Philadelphia, Pa.
13. **Collins, J. E., P. K. Legan, T. P. Kenny, J. MacGarvie, J. L. Holton, and D. R. Garrod.** 1991. Cloning and sequence analysis of desmosomal glycoproteins 2 and 3 (desmocollins): cadherin-like desmosomal adhesion molecules with heterogeneous cytoplasmic domains. J. Cell Biol. **113:**381–391.
14. **Cudmore, S., I. Reckmann, and M. Way.** 1997. Viral manipulations of the actin cytoskeleton. Trends Microbiol. **5:**142–148.
15. **Dingwell, K. S., C. R. Brunetti, R. L. Hendricks, Q. Tang, M. Tang, A. J. Rainbow, and D. C. Johnson.** 1994. Herpes simplex virus glycoproteins E and I facilitate cell-to-cell spread in vivo and across junctions of cultured cells. J. Virol. **68:**834–845.
16. **Dingwell, K. S., L. C. Doering, and D. C. Johnson.** 1995. Glycoproteins E and I facilitate neuron-to-neuron spread of herpes simplex virus. J. Virol. **69:**7087–7098.
17. **Dingwell, K. S., and D. C. Johnson.** 1998. The herpes simplex virus gE-gI complex facilitates cell-to-cell spread and binds to components of cell junctions. J. Virol. **72:**8933–8942.
18. **Duus, K. M., and C. Grose.** 1996. Multiple regulatory effects of varicella-zoster virus (VZV) gL on trafficking patterns and fusogenic properties of VZV gH. J. Virol. **70:**8961–8971.
19. **Duus, K. M., C. Hatfield, and C. Grose.** 1995. Cell surface expression and fusion by the varicella-zoster virus gH:gL glycoprotein complex: analysis by laser scanning confocal microscopy. Virology **210:**429–440.
20. **Gershon, A. A., D. L. Sherman, Z. Zhu, C. A. Gabel, R. T. Ambron, and M. D. Gershon.** 1994. Intracellular transport of newly synthesized varicella-zoster virus: final envelopment in the trans-Golgi network. J. Virol. **68:**6372–6390.
21. **Gonzalez-Mariscal, L., B. Chavez de Ramirez, and M. Cereijido.** 1985. Tight junction formation in cultured epithelial cells (MDCK). J. Membr. Biol. **86:**113–125.
22. **Gonzalez, M. L., S. Islas, R. G. Contreras, V. M. Garcia, A. Betanzos, J. Vega, Q. A. Diaz, O. N. Martin, N. V. Ortiz, M. Cereijido, and J. Valdes.** 1999. Molecular characterization of the tight junction protein ZO-1 in MDCK cells. Exp. Cell Res. **248:**97–109.
23. **Grindstaff, K. K., R. L. Bacallao, and W. J. Nelson.** 1998. Apiconuclear organization of microtubules does not specify protein delivery from the trans-Golgi network to different membrane domains in polarized epithelial cells. Mol. Biol. Cell **9:**685–699.
24. **Grose, C.** 1990. Glycoproteins encoded by varicella-zoster virus: biosynthesis, phosphorylation, and intracellular trafficking. Annu. Rev. Microbiol. **44:**59–80.
25. **Gumbiner, B.** 1991. Cell adhesion molecules in epithelia, p. 91–104. *In* M. Cereijido (ed.), Tight junctions. CRC Press, Boca Raton, Fla.
26. **Gumbiner, B., B. Stevenson, and A. Grimaldi.** 1988. The role of the cell adhesion molecule uvomorulin in the formation and maintenance of the epithelial junctional complex. J. Cell Biol. **107:**1575–1587.
27. **Itoh, M., A. Nagafuchi, S. Yonemura, Y. T. Kitani, S. Tsukita, and S. Tsukita.** 1993. The 220-kD protein colocalizing with cadherins in non-epithelial cells is identical to ZO-1, a tight junction-associated protein in epithelial cells: cDNA cloning and immunoelectron microscopy. J. Cell Biol. **121:**491–502.
28. **Jou, T. S., E. E. Schneeberger, and W. J. Nelson.** 1998. Structural and functional regulation of tight junctions by RhoA and Rac1 small GTPases. J. Cell Biol. **142:**101–115.
29. **Knapp, A. C., P. J. Husak, and L. W. Enquist.** 1997. The gE and gI homologs from two alphaherpesviruses have conserved and divergent neuroinvasive properties. J. Virol. **71:**5820–5827.
30. **Kritas, S. K., H. J. Nauwynck, and M. B. Pensaert.** 1995. Dissemination of wild-type and gC-, gE- and gI-deleted mutants of Aujeszky's disease virus in the maxillary nerve and trigeminal ganglion of pigs after intranasal inoculation. J. Gen. Virol. **76:**2063–2066.
31. **Litwin, V., W. Jackson, and C. Grose.** 1992. Receptor properties of two varicella-zoster virus glycoproteins, gpI and gpIV, homologous to herpes simplex virus gE and gI. J. Virol. **66:**3643–3651.
32. **Madara, J. L., and K. Dharmsathaphorn.** 1985. Occluding junction structure-function relationships in a cultured epithelial monolayer. J. Cell Biol. **101:**2124–2133.
33. **Maidji, E., S. Tugizov, G. Abenes, T. Jones, and L. Pereira.** 1998. A novel human cytomegalovirus glycoprotein, gpUS9, which promotes cell-to-cell spread in polarized epithelial cells, colocalizes with the cytoskeletal proteins E-cadherin and F-actin. J. Virol. **72:**5717–5727.
34. **Maidji, E., S. Tugizov, T. Jones, Z. Zheng, and L. Pereira.** 1996. Accessory human cytomegalovirus glycoprotein US9 in the unique short component of the viral genome promotes cell-to-cell transmission of virus in polarized epithelial cells. J. Virol. **70:**8402–8410.
35. **Mallory, S., M. Sommer, and A. M. Arvin.** 1997. Mutational analysis of the role of glycoprotein I in varicella-zoster virus replication and its effects on glycoprotein E conformation and trafficking. J. Virol. **71:**8279–8288.
36. **Mays, R. W., K. A. Siemers, B. A. Fritz, A. W. Lowe, G. van Meer, and W. J. Nelson.** 1995. Hierarchy of mechanisms involved in generating Na/K-ATPase polarity in MDCK epithelial cells. J. Cell Biol. **130:**1105–1115.
37. **Mitic, L. L., E. E. Schneeberger, A. S. Fanning, and J. M. Anderson.** 1999. Connexin-occludin chimeras containing the ZO-binding domain of occludin localize at MDCK tight junctions and NRK cell contacts. J. Cell Biol. **146:**683–693.
38. **Nagafuchi, A., and M. Takeichi.** 1988. Cell binding function of E-cadherin is regulated by the cytoplasmic domain. EMBO J. **7:**3679–3684.
39. **Nathke, I. S., L. Hinck, J. R. Swedlow, J. Papkoff, and W. J. Nelson.** 1994. Defining interactions and distributions of cadherin and catenin complexes in polarized epithelial cells. J. Cell Biol. **125:**1341–1352.
40. **Nelson, W. J.** 1992. Regulation of cell surface polarity from bacteria to mammals. Science **258:**948–955.
41. **Ojakian, G. K., and R. Schwimmer.** 1988. The polarized distribution of an apical cell surface glycoprotein is maintained by interaction with the cytoskeleton of Madin-Darby canine kidney cells. J. Cell Biol. **107:**2377–2387.
42. **Olson, J. K., G. A. Bishop, and C. Grose.** 1997. Varicella-zoster virus Fc receptor gE glycoprotein: serine/threonine and tyrosine phosphorylation of monomeric and dimeric forms. J. Virol. **71:**110–119.
43. **Olson, J. K., and C. Grose.** 1998. Complex formation facilitates endocytosis of the varicella-zoster virus gE:gI Fc receptor. J. Virol. **72:**1542–1551.
44. **Olson, J. K., and C. Grose.** 1997. Endocytosis and recycling of varicella-zoster virus Fc receptor glycoprotein gE: internalization mediated by a YXXL motif in the cytoplasmic tail. J. Virol. **71:**4042–4054.
45. **Overduin, M., T. S. Harvey, S. Bagby, K. I. Tong, P. Yau, M. Takeichi, and M. Ikura.** 1995. Solution structure of the epithelial cadherin domain responsible for selective cell adhesion. Science **267:**386–389.
46. **Ozawa, M., H. Baribault, and R. Kemler.** 1989. The cytoplasmic domain of the cell adhesion molecule uvomorulin associates with three independent proteins structurally related in different species. EMBO J. **8:**1711–1717.
47. **Rimm, D. L., E. R. Koslov, P. Kebriaei, C. D. Cianci, and J. S. Morrow.** 1995. Alpha 1 (E)-catenin is an actin-binding and -bundling protein mediating the attachment of F-actin to the membrane adhesion complex. Proc. Natl. Acad. Sci. USA **92:**8813–8817.
48. **Rodriguez-Boulan, E., and S. K. Powell.** 1992. Polarity of epithelial and neuronal cells. Annu. Rev. Cell Biol. **8:**395–427.
49. **Schneeberger, E. E., and R. D. Lynch.** 1992. Structure, function, and regulation of cellular tight junctions. Am. J. Physiol. **262:**L647–L661.
50. **Staehelin, L. A.** 1974. Structure and function of intercellular junctions. Int. Rev. Cytol. **39:**191–284.
51. **Stevenson, B. R., J. M. Anderson, D. A. Goodenough, and M. S. Mooseker.** 1988. Tight junction structure and ZO-1 content are identical in two strains of Madin-Darby canine kidney cells which differ in transepithelial resistance. J. Cell Biol. **107:**2401–2408.
52. **Takeichi, M.** 1990. Cadherins: a molecular family important in selective cell-cell adhesion. Annu. Rev. Biochem. **59:**237–252.

53. **Tirabassi, R. S., and L. W. Enquist.** 1999. Mutation of the YXXL endocytosis motif in the cytoplasmic tail of pseudorabies virus gE. J. Virol. **73:**2717–2728.
54. **Tsukita, S., and M. Furuse.** 2000. Pores in the wall: claudins constitute tight junction strands containing aqueous pores. J. Cell Biol. **149:**13–16.
55. **Wang, Z., M. D. Gershon, O. Lungu, C. A. Panagiotidis, Z. Zhu, Y. Hao, and A. A. Gershon.** 1998. Intracellular transport of varicella-zoster glycoproteins. J. Infect. Dis. **178**(Suppl. 1)**:**S7–S12.
56. **Whealy, M. E., J. P. Card, A. K. Robbins, J. R. Dubin, H. J. Rziha, and L. W. Enquist.** 1993. Specific pseudorabies virus infection of the rat visual system requires both gI and gp63 glycoproteins. J. Virol. **67:**3786–3797.
57. **Yap, A. S., C. M. Niessen, and B. M. Gumbiner.** 1998. The juxtamembrane region of the cadherin cytoplasmic tail supports lateral clustering, adhesive strengthening, and interaction with p120ctn. J. Cell Biol. **141:**779–789.
58. **Zhu, Z., M. D. Gershon, Y. Hao, R. T. Ambron, C. A. Gabel, and A. A. Gershon.** 1995. Envelopment of varicella-zoster virus: targeting of viral glycoproteins to the trans-Golgi network. J. Virol. **69:**7951–7959.
59. **Zhu, Z., Y. Hao, M. D. Gershon, R. T. Ambron, and A. A. Gershon.** 1996. Targeting of glycoprotein I (gE) of varicella-zoster virus to the trans-Golgi network by an AYRV sequence and an acidic amino acid-rich patch in the cytosolic domain of the molecule. J. Virol. **70:**6563–6575.